

# Indium Tin Oxide Template Development for Step and Flash Imprint Lithography

Kathleen A. Gehoski<sup>a</sup>, Douglas J. Resnick\*<sup>a</sup>, William J. Dauksher<sup>a</sup>, Kevin J. Nordquist<sup>a</sup>, Eric Ainley<sup>a</sup>, Mark McCord<sup>b</sup>, Mark, Raphaelian, Harald Hess<sup>b</sup>

<sup>a</sup>Embedded Systems and Physical Sciences Labs, Motorola, 2100 E. Elliot Rd., Tempe, AZ 85284

<sup>b</sup>KLA-Tencor, 160 Rio Robles, San Jose, CA 95134

## ABSTRACT

Step and Flash Imprint Lithography (SFIL) is an attractive method for printing sub-100 nm geometries. Relative to other imprinting processes SFIL has the advantage that the template is transparent, thereby facilitating conventional overlay techniques. Previous work on S-FIL templates has focused on a chromium and quartz pattern transfer process that is compatible with processes that are currently used in mask shops. It is likely that 1X templates will require electron beam inspection, however, and templates that include buried charge conduction layers may be required. The purpose of this work was to investigate the issues associated with fabricating and inspecting these types of templates. The patterning stack examined included a layer of ZEP-520 positive electron beam resist, followed by thin layers of chromium, silicon oxynitride, and indium tin oxide. The chromium layer was needed to avoid laser height sensor problems encountered prior to electron beam exposure. The pattern transfer process was characterized and CD uniformity was characterized in four quadrants of the photoplate. A prototype electron beam inspection system was then used to inspect an array of programmed defect patterns. Conclusions from the pattern inspection work needed here. Two methods for fabricating templates were considered.

Keywords: Imprint, S-FIL, electron beam, inspection, ITO, template

## 1. INTRODUCTION

Imprint lithography is attracting attention as a low cost method for printing nanometer scale geometries. Although imprint lithography has been primarily used in research and development environments, Sematech has recently placed imprint lithography on the International Technology Roadmap for Semiconductors (ITRS roadmap) as a potential lithography method at the 32 and 22 nm fabrication nodes. Step and Flash Imprint Lithography (S-FIL) is a particularly attractive imprint method for printing sub-100 nm geometries [1-3]. In order for S-FIL technology to successfully make the transition from research and development to a viable manufacturing processing technique suitable for fabricating high density circuits, a 1X template infrastructure needs to be both defined and supported. It is critical, therefore, that templates are compatible with state of the art inspection tools. For 1X technology, the best choice for inspection is likely to be an electron beam based system.

In this work, templates were prepared by depositing an Indium Tin Oxide (ITO) layer, and a silicon oxynitride film. Relief images were formed by patterning ZEP 520 resist, and transferring the patterns into the oxynitride layer, stopping on the ITO. Two key issues need to be addressed in order to make this a viable process. With respect to the fabrication process, the material stack on the photoplate must be compatible with the laser height sensor of the electron beam writer. In addition, the final patterns must have sufficient contrast in an electron beam based inspection system to allow for the detection of defects.

We report on the processes developed to fabricate the templates, and will discuss the methods developed for enabling repeatable imprinting and inspection.

Email: Kathy.gehoski@motorola.com Phone: 480 413-7262 Fax: 480 413-5453

\* Current email address: dresnick@molecularimprints.com

## 2. EXPERIMENTAL DETAILS

For the fabrication of templates, 15 nm of sputter deposited chromium (Cr), 100 nm PECVD (plasma enhanced chemical vapor deposition)  $\text{SiO}_x\text{N}_y$  and 60 nm indium tin oxide (ITO) films were deposited on 6" x 6" x 0.25" photomask substrates. ZEP520A resist spun to a thickness of 160 nm was imaged on a Leica VB-6 HR electron beam exposure system operating at 100 keV. The actual patterns were written in four 25 mm x 25 mm areas centered in each of four quadrants on a 6025 plate. The Cr films were etched using chlorine and oxygen in a Unaxis VLR. The oxynitride films were pattern transferred using a  $\text{CF}_4$ -based RIE process in a Unaxis VLR. The remaining e-beam resist was stripped in a conventional barrel asher.

The ITO films themselves were deposited in a Motorola-designed three cathode sputtering system equipped with both RF and DC sputter capabilities. In this system, the substrate holder is located above the cathodes, and the system base pressure is  $5.0 \times 10^{-7}$  Torr. No pre-sputter surface preparation was performed on the substrates. All depositions were conducted at 3 mT. In order to maximize optical transmission at 365 nm and to lower resistivity, the ITO films were annealed on a hot plate at 350 °C. The ITO film characteristics have been previously reported [4,5].

Templates were cleaned and treated using isopropyl alcohol. A Branson 8000 oxygen asher was also used to remove organic materials from template surfaces. Templates were coated with a RelMat™ release agent. A photosensitive imaging layer of 9 wt% Si was imprinted on the wafers with the patterned template using an Imprio 100™ tool manufactured by Molecular Imprints, Inc. Inspection was performed using a prototype e-beam inspection system of the KLA-Tencor eS30.

## 3. PATTERN TRANSFER PROCESS

### 3.1 Writing Issues

An etch process incorporating an ITO film has previously been reported. The pattern transfer scheme is schematically depicted below (see Figure 1). ZEP520 is exposed with a dose of 800 – 900  $\mu\text{C}/\text{cm}^2$ . After a short descum, the oxynitride film is etched in  $\text{CF}_4$ , stopping on the ITO. An etch stop approach is advantageous for two reasons: (1) With an appropriate overetch, all features have an identical etch depth. (2) The overetch also eliminates the notching observed for templates consisting of Cr and quartz.

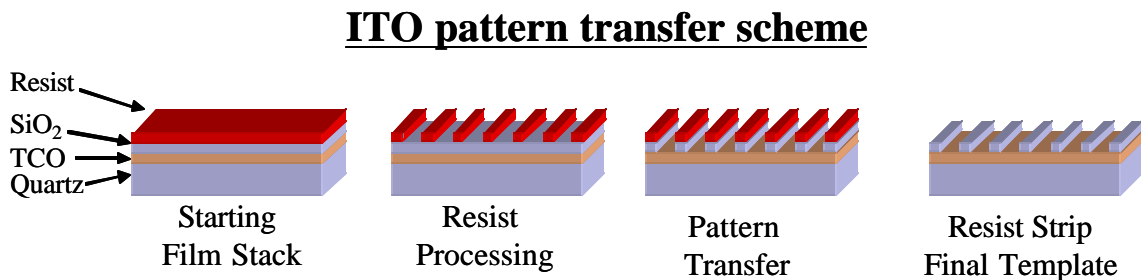


Figure 1. Pattern transfer scheme for a stack containing a transparent conducting oxide film.

Results with the stack shown above have been inconsistent. The reason is related to the process used by the Leica VB6 to detect the writing surface of the template. A laser height sensor uses laser diode linearly polarized light at 780 nm and it is oriented so that the polarization is in the horizontal plane. The angle of the light on the surface of the resist is about 22 degrees. The reflected signal is collected on a position detector. By measuring several points across the plate,

it is possible to map the flatness of the plate, determine the optimal writing distance to minimize beam size, and correct the writing grid when non-flat areas are encountered.

Problems occur when the substrate is transparent or semi-transparent, as is the case for a plate with an SiO<sub>x</sub>N<sub>y</sub>/ITO material stack. Reflections can now occur at the various interfaces, as well as from the bottom of the plate, causing a broadening in the reflected signal intensity. An example of this effect is shown in Figure 2. Figure 2a depicts the signal intensity from a plate coated with 15 nm of Cr. Figure 2b depicts the signal from a plate coated with ITO and SiO<sub>x</sub>N<sub>y</sub>. Note the difference in the width of the two peaks. The broadening observed in Figure 2b results in errors of the height mapping algorithm, thereby causing field to field butting errors.

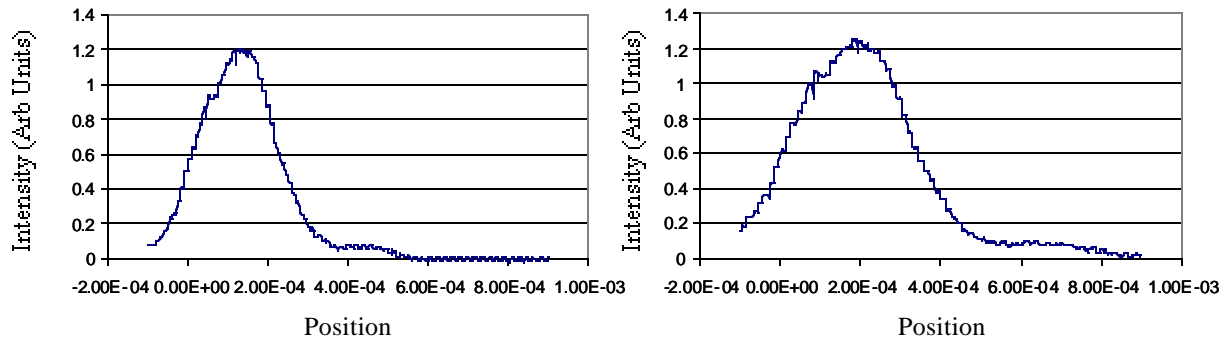


Figure 2. (a) Laser signal intensity from the surface of a quartz plate coated with a 15 nm Cr film. (b) Laser signal intensity from a plate coated with 60 nm of ITO followed by 100 nm of SiO<sub>x</sub>N<sub>y</sub>.

The problem is resolved by adding an additional 15 nm Cr layer on top of the SiO<sub>x</sub>N<sub>y</sub> film. Although the etch stack is more complex, the reflected signal from the laser is now very similar to the one shown in Figure 2a. In addition, the advantages associated with the ITO etch stop layer are still maintained. The new pattern transfer scheme is shown in Figure 3.

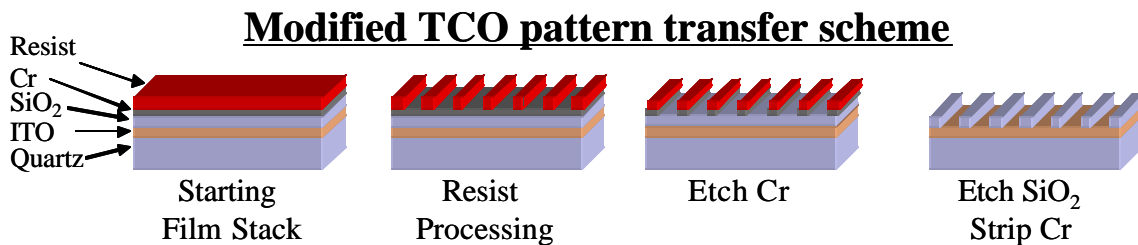


Figure 3. Butting errors encountered when patterning a semi-transparent plate are eliminated by adding a 15 nm Cr film to the material stack.

### 3.2 Pattern Transfer: Process Latitude and Uniformity

Patterning and pattern transfer consists of three main process steps: Resist exposure and descum, Cr etch and resist strip, and an SiO<sub>x</sub>N<sub>y</sub> etch followed by a wet strip of the Cr. To understand process latitude, the four quadrants of a photoplate were exposed with a resolution test pattern at doses ranging from 850 μC/cm<sup>2</sup> to 1000 μC/cm<sup>2</sup> in steps of 50 μC/cm<sup>2</sup>. Critical dimensions were measured after the key process steps described above. The resulting images are displayed in Figure 4.

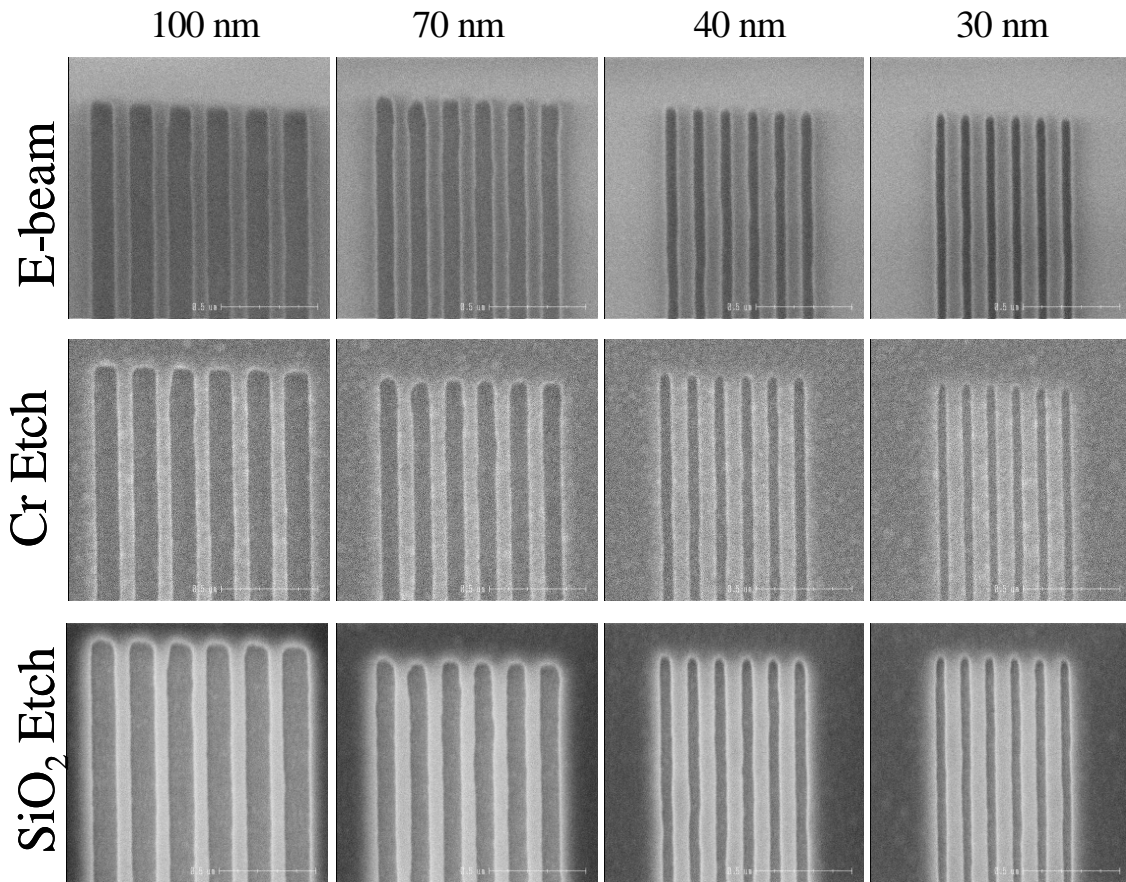


Figure 4. 100 nm, 70 nm, 40, and 30 nm trenches after resist exposure and development, Cr etch , and quartz etch.

It is interesting to note that the exposure latitude degrades during the pattern transfer process. Very little CD variation is evident after the exposure and develop process. After the quartz etch, however, a difference of up to 10 nm is observed between the lowest ( $850 \mu\text{C}/\text{cm}^2$ ) exposure dose, and the highest exposure dose ( $1000 \mu\text{C}/\text{cm}^2$ ). One possible explanation is that although the measured CDs are very similar after exposure and develop, the wall profile of the feature is changed, leading to increases in the CD after etch.

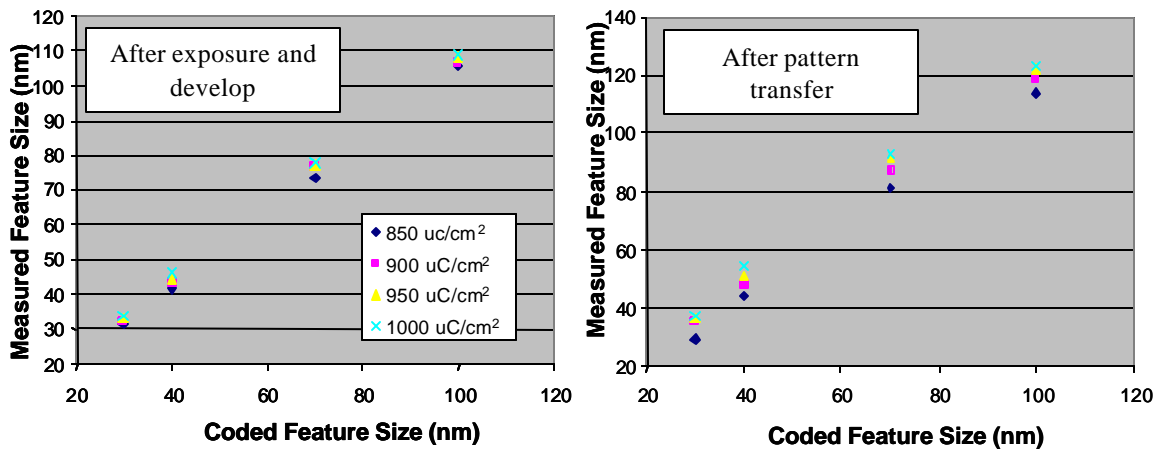


Figure 5. Coded vs. measured feature size of 100 nm, 70 nm, 40 nm, and 30 nm trenches after exposure and after pattern transfer.

It is also interesting to compare the final features on an ITO-based template and a Cr/Quartz template. Figure 6a depicts 100 nm and 40 nm images taken from the two types of templates. Figure 6b compares final feature sizes from both types of templates. Plotted are the 100 nm, 70 nm, 40 nm, and 30 nm semi-dense features as a function of coded feature size. Because of proximity effects, the larger features are have measured values approximately 10 nm too big, while the smallest features are very close to their coded values. Because the pattern transfer process parameters are essentially the same, the comparable dimensions for both types of templates are not unexpected.

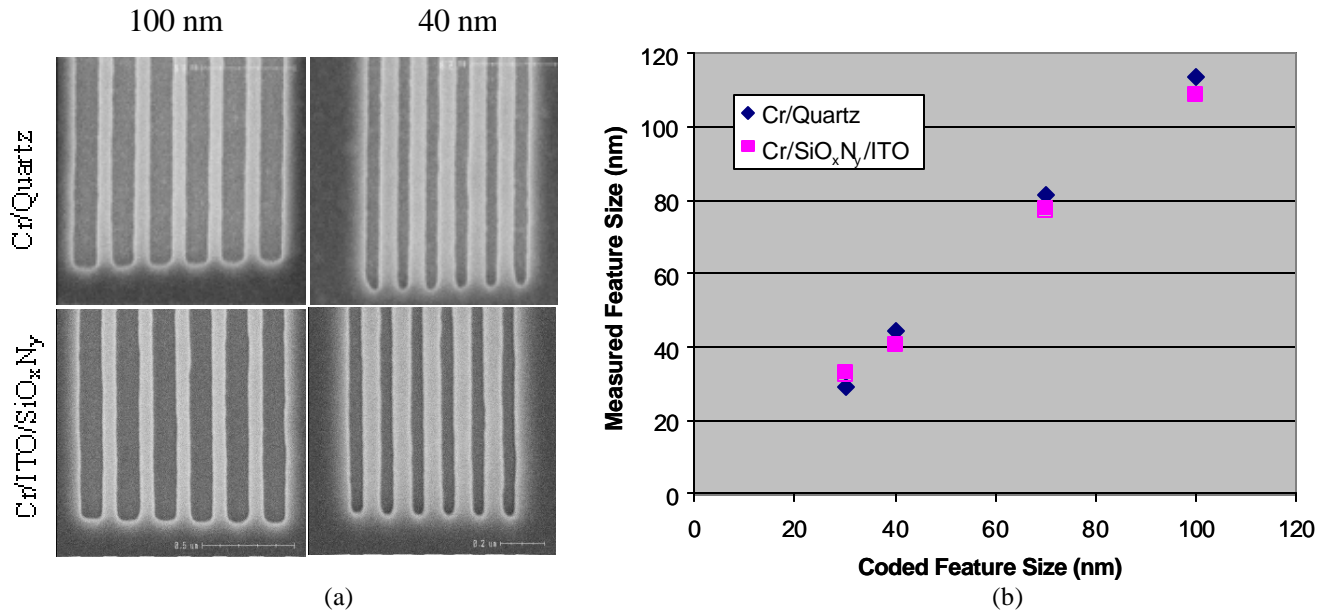


Figure 6. Comparison of a finished Cr/Quartz and Cr/SiO<sub>x</sub>N<sub>y</sub>/ITO template features. Because the exposure and etch processes are similar, final feature sizes are very comparable.

Feature size uniformity was measured by exposing the same patterns in all four quadrants of the photoplate and comparing final feature size. The results are shown in Figure 7 below. Figure 7a depicts 40 nm semi-dense trenches from each quadrant. Figure 7b contains feature size data from all four quadrants. The average 3σ variation was 4.7 nm, which is very comparable to uniformity data obtained from Cr/Quartz templates [7].

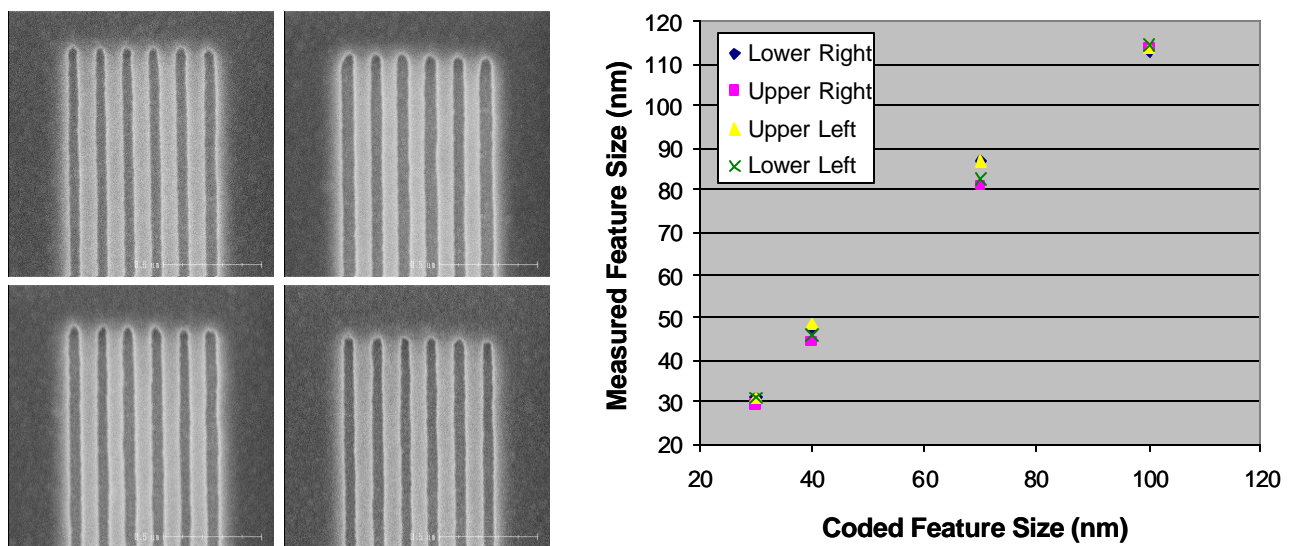


Figure 7. (a) 40 nm from all four quadrants. (b) Coded vs. Measured size for 100 nm, 70 nm, 40 nm, and 30 nm features.

#### 4. ELECTRON BEAM INSPECTION

Previous electron beam work established that programmed defects patterned on an ITO-based template can be calibrated in a CD SEM and inspected on a prototype e-beam inspection system of the KLA -Tencor eS30m [8,9]. The initial images Figure 8 (left) confirmed that these ITO templates are inspectable. This means that two important issues were addressed: the contrast is excellent and surface charging does not seem to be an issue with the transparent oxide conductors.

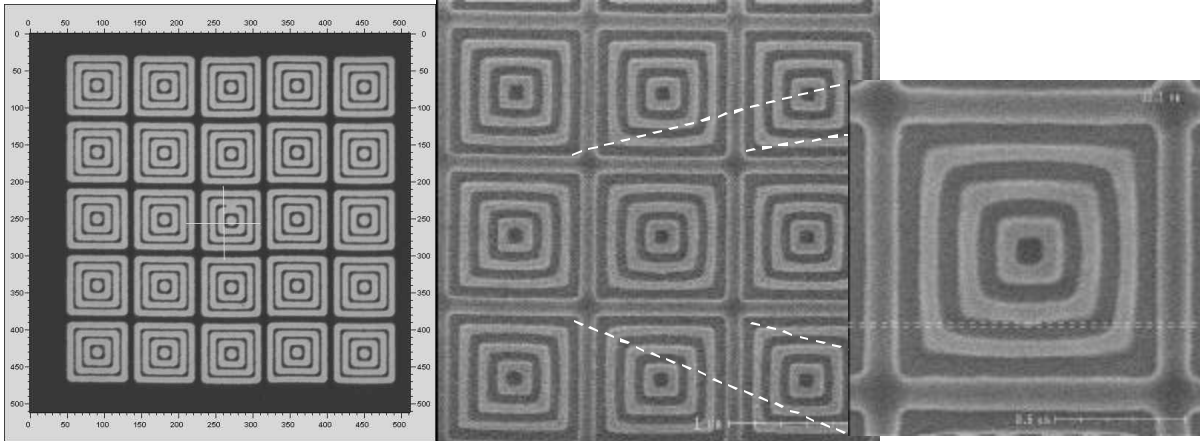


Fig 8. E-beam inspection picture of 400 nm pattern made on ITO template(left). It shows excellent contrast and no charging effects. A CDSEM image showing 13 nm programmed line edge defect on 70 nm test cell(center and right).

This work was done, however, on a 6025 photoplate, prior to the formation of the pedestal regions. When the pedestals are formed after patterning, the ITO outside the pedestal area is removed. The process is shown schematically in Figure 9. Templates were prepared by writing programmed defect patterns in each quadrant of the plate, completing the pattern transfer, and forming the pedestals. The final template, with ITO only remaining on the pedestal was inserted into the prototype e-beam inspection tool to understand whether an ungrounded ITO film was sufficient for dissipating charge.

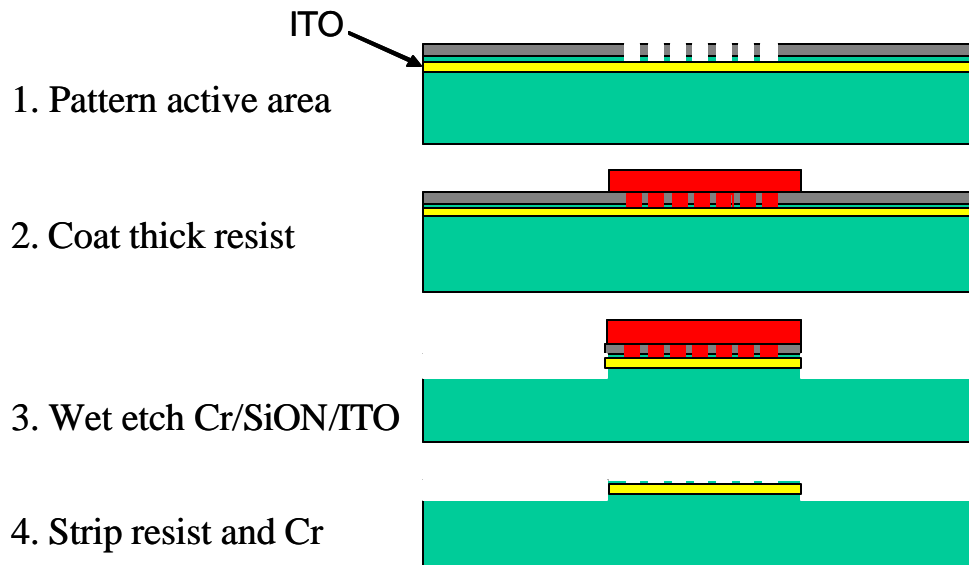


Figure 9. Schematic illustration of the process used to define the pedestal area on a 6025 plate.

A variety of different types of programmed defects, along with reference die were created for the inspection process. An example of a programmed defect, with a size ranging from 70 nm to 400 nm is shown in Figure 10.

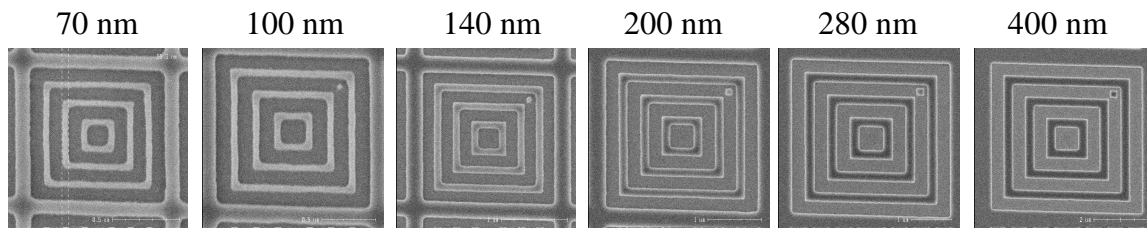


Figure 10. A programmed defect located towards the upper right corner of the cell. Defect size ranged from 70 nm to 400 nm.

The ITO templates were imaged in an eS31 electron beam inspection machine. Sample swaths of the programmed defect areas were collected at a landing energy of 1000eV, a pixel size of 50 nm, and a pixel rate of 200 MHz. The 140 nm features and their programmed defects were readily resolved. Within a swath, image brightness and contrast was relatively stable and free of charging artifacts. However, contrast did tend to vary with time. In these tests, the ITO layer was left floating, and the ITO layer was probably charging over time. Future experiments will provide electrical connection between the ITO layer and the stage to confirm that long-term stable imaging can be obtained. Examples of the 140 nm features are shown below in Figure 11.

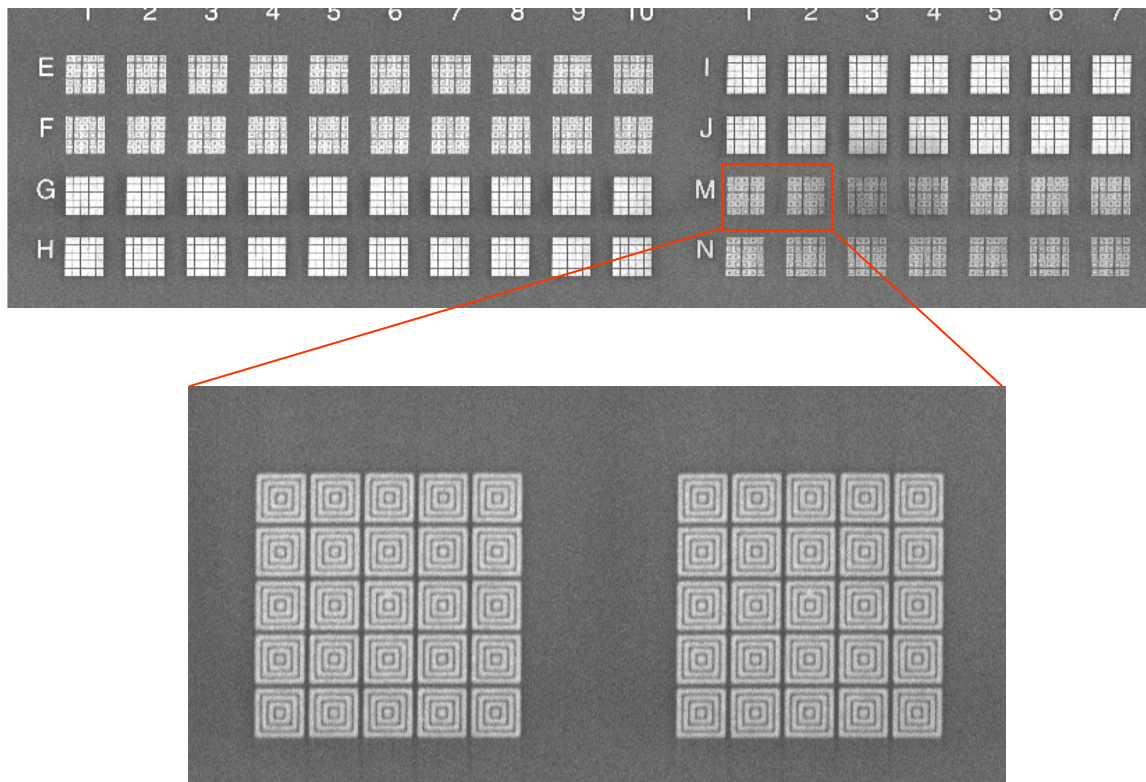


Figure 11. The 140nm features and their programmed defects.

## 5. CONCLUSIONS

Two different methods have been used to produce high-resolution templates suitable for Step and Flash Imprint Lithography. Template features as small as 20 nm were obtained by switching to ZEP-520 resist and using a very thin Cr film as the hardmask. The smallest features in the template were also successfully printed. Proof of concept for employing a transparent conductive oxide as an etch stop has also been demonstrated. Printed 65 nm features were resolved. It is expected that better resolution will be obtained when the ITO/SiO<sub>2</sub> process is transferred to quartz plates. Future work will focus on further optimization of the ITO films. New work will also be started to examine the issues associated with fabricating simple devices.

## ACKNOWLEDGEMENTS

The authors gratefully acknowledge Steve Smith, Dolph Rios, Eric Newlin, and David Standfast, for their process help. We would also like to thank Lester Casoose, Kathy Palmer, and Mark Madrid for their characterization work. Finally, we thank Papu Maniar and Vida Ilderem for their support. This work was partially funded by DARPA (N66001-02-C-8011) and the NIST-ATP (96-LC-460).

## REFERENCES

1. T. Bailey, B. J. Choi, M. Colburn, M. Meissl, S. Shaya, J. G. Ekerdt, S. V. Sreenivasan, and C. G. Willson, *J. Vac. Sci. Technol. B* 18(6), 3572 (2000).
2. M. Colburn, S. Johnson, M. Stewart, S. Damle, T. Bailey, B. Choi, M. Wedlake, T. Michaelson, S. V. Sreenivasan, J. Ekerdt, and C. G. Willson, *Proc. SPIE, Emerging Lithographic Technologies III*, 379 (1999).
3. M. Colburn, T. Bailey, B. J. Choi, J. G. Ekerdt, S. V. Sreenivasan, *Solid State Technology*, 67, June 2001.
4. T. C. Bailey, D. J. Resnick, D. Mancini, K. J. Nordquist, W. J. Dauksher, E. Ainley, A. Talin, K. Gehoski, J. H. Baker, B. J. Choi, S. Johnson, M. Colburn, M. Meissl, S. V. Sreenivasan, J. G. Ekerdt, and C. G. Willson, *Microelectronic Engineering* 2002,
5. A. E. Hooper, A. A. Talin, D. J. Resnick, J. H. Baker, D. Convey, T. Eschrich, H. G. Tompkins, and W. J. Dauksher, *6. Proceedings, Nanotech 2003, Volume 3*, 47 – 50.
6. W. J. Dauksher, K. J. Nordquist, D. P. Mancini, D. J. Resnick, J. H. Baker, A. E. Hooper, A. A. Talin, T. C. Bailey, A. M. Lemonds, S. V. Sreenivasan, J. G. Ekerdt, and C. G. Willson, *J. Vac. Sci. Technol. B* 20(6), Nov/Dec 2002, 2857 – 2861.
7. David P. Mancini, Kathleen A. Gehoski, William J. Dauksher, Kevin J. Nordquist, and Douglas J. Resnick, *Proc., SPIE Emerging Lithographic Technologies VII*, 187 (2003).
8. Harald F. Hess, Don Pettibone, David Adler, and Kirk Bertsche, Kevin J. Nordquist, David P. Mancini, William J. Dauksher, and Douglas J. Resnick, *J. Vac. Sci. Technol. B* 22(6), Nov/Dec 2004, 3300 – 3305.
9. Kevin J. Nordquist, William J. Dauksher, David P. Mancini, Douglas J. Resnick, Harald F. Hess, Donald W. Pettibone, David Adler, Kirk Bertsche, Roy White, Jeffrey E. Csuy, and David Lee, *Proc. SPIE Vol. 5567*, p. 853-863 (2004).